Isolator-Free Switchable Uni- and Bidirectional hybrid mode-locked erbium-doped fiber laser

Maria Chernysheva,[1,*] **Mohammed Al Araimi,**[1,2] **Hani Kbashi,**[1]**, Raz Arif,**[3] **Sergey V. Sergeyev,**[1] **and Aleksey Rozhin**[1]

[1]*Nanoscience Research Group and Aston Institute of Photonic Technologies, Aston University, Birmingham, B4 7ET, UK*
[2]*Al Musanna College of Technology, Muladdah, Al Musanna, Sultanate of Oman*
[3]*Physics Department, University of Sulaimani, Sulaimani, Iraq*
[*]*m.chernysheva@aston.ac.uk*

Abstract: An Erbium-doped fibre ring laser hybrid mode-locked with single-wall carbon nanotubes (SWNT) and nonlinear polarisation evolution (NPE) without an optical isolator has been investigated for various cavity conditions. Precise control of the state of polarisation (SOP) in the cavity ensures different losses for counter-propagating optical fields. As the result, the laser operates in quasi-unidirectional regime in both clockwise (CW) and counter-clockwise (CCW) directions with the emission strengths difference of the directions of 22 dB. Furthermore, by adjusting the net birefringence in the cavity, the laser can operate in a bidirectional generation. In this case, laser pumped with 75 mW power at 980 nm generates almost identical 790 and 570 fs soliton pulses with an average power of 1.17 and 1.11 mW. The operation stability and pulse quality of the soliton pulses in both unidirectional regimes are highly competitive with those generated in conventional ring fibre lasers with isolator in the cavity. Demonstrated bidirectional laser operation can find vital applications in gyroscopes or precision rotation sensing technologies.

OCIS codes: (060.3510) Lasers, fiber; (140.4050) Mode-locked lasers; (190.4370) Nonlinear optics, fibers.

References and links

1. U. Keller, "Recent developments in compact ultrafast lasers." Nature **424**, 831–8 (2003).
2. T. Hasan, Z. Sun, F. Wang, F. Bonaccorso, P. H. Tan, A. G. Rozhin, and A. C. Ferrari, "Nanotube-Polymer Composites for Ultrafast Photonics," Advanced Materials **21**, 3874–3899 (2009).
3. M. Chernysheva, A. Rozhin, Y. Fedotov, C. Mou, R. Arif, S. M. Kobtsev, E. M. Dianov, and S. K. Turitsyn, "Carbon nanotubes for ultrafast fibre lasers," Nanophotonics (2016).
4. Z. Sun, T. Hasan, F. Torrisi, D. Popa, G. Privitera, F. Wang, F. Bonaccorso, D. M. Basko, and A. C. Ferrari, "Graphene mode-locked ultrafast laser." ACS Nano **4**, 803–10 (2010).
5. R. I. Woodward, R. C. T. Howe, T. H. Runcorn, G. Hu, F. Torrisi, E. J. R. Kelleher, and T. Hasan, "Wideband saturable absorption in few-layer molybdenum diselenide (MoSe$_2$) for Q-switching Yb-, Er- and Tm-doped fiber lasers." Optics Express **23**, 20051–61 (2015).
6. E. G. Lariontsev and V. N. Serkin, "Possibility of using self-focusing for increasing contrast and narrowing of ultrashort light pulses," Soviet Journal of Quantum Electronics **5**, 796–800 (1975).
7. N. J. Doran and D. Wood, "Nonlinear-optical loop mirror," Optics Letters **13**, 56 (1988).
8. M. E. Fermann, F. Haberl, M. Hofer, and H. Hochreiter, "Nonlinear amplifying loop mirror," Optics Letters **15**, 752 (1990).

9. F. Kurtner, J. der Au, and U. Keller, "Mode-locking with slow and fast saturable absorbers-what's the difference?" IEEE Journal of Selected Topics in Quantum Electronics **4**, 159–168 (1998).
10. M. A. Chernysheva, A. A. Krylov, R. N. Arif, A. G. Rozhin, M. H. Rummelli, S. K. Turitsyn, and E. M. Dianov, "Higher-Order Soliton Generation in Hybrid Mode-Locked Thulium-Doped Fiber Ring Laser," IEEE Journal of Selected Topics in Quantum Electronics **20**, 425–432 (2014).
11. D. S. Chernykh, A. A. Krylov, A. E. Levchenko, V. V. Grebenyukov, N. R. Arutunyan, A. S. Pozharov, E. D. Obraztsova, and E. M. Dianov, "Hybrid mode-locked erbium-doped all-fiber soliton laser with a distributed polarizer." Applied optics **53**, 6654–62 (2014).
12. D. Gnass, N. Ernsting, and F. Schaefer, "Sagnac effect in the colliding-pulse-mode-locked dye ring laser," Applied Physics B - Photophysics and Laser Chemistry (ISSN 0721-7269) (1991).
13. W. R. Christian and M. J. Rosker, "Picosecond pulsed diode ring-laser gyroscope." Optics letters **16**, 1587–9 (1991).
14. M. L. Dennis, J.-C. M. Diels, and M. Lai, "Femtosecond ring dye laser: a potential new laser gyro," Optics Letters **16**, 529 (1991).
15. Y. Liu, L. Sun, H. Qiu, Y. Wang, Q. Tian, and X. Ma, "Bidirectional operation and gyroscopic properties of passively mode-locked Nd:YVO 4 ring laser," Laser Physics Letters **4**, 187–190 (2007).
16. M. Y. Jeon, H. J. Jeong, and B. Y. Kim, "Mode-locked fiber laser gyroscope," Optics Letters **18**, 320 (1993).
17. B. W. Lee, H. J. Jeong, and B. Y. Kim, "High-sensitivity mode-locked fiber laser gyroscope," Optics Letters **22**, 129 (1997).
18. D. Chernykh and A. Krylov, "Gyroscopic effect in the bidirectional femtosecond erbium-doped fiber ring laser," International Conference on Lasers Optics 2014 (2014).
19. K. Tamura, J. Jacobson, E. P. Ippen, H. A. Haus, and J. G. Fujimoto, "Unidirectional ring resonators for self-starting passively mode-locked lasers," Optics Letters **18**, 220 (1993).
20. E. H. Turner and R. H. Stolen, "Fiber Faraday circulator or isolator." Optics letters **6**, 322–3 (1981).
21. D. Jalas, A. Petrov, M. Eich, W. Freude, S. Fan, Z. Yu, R. Baets, M. Popović, A. Melloni, J. D. Joannopoulos, M. Vanwolleghem, C. R. Doerr, and H. Renner, "What is and what is not an optical isolator," Nature Photonics **7**, 579–582 (2013).
22. Y. Shi, M. Sejka, and O. Poulsen, "A unidirectional Er/sup 3+/-doped fiber ring laser without isolator," IEEE Photonics Technology Letters **7**, 290–292 (1995).
23. W. Lai, P. Shum, and L. Binh, "NOLM-NALM fiber ring laser," IEEE Journal of Quantum Electronics **41**, 986–993 (2005).
24. S. Kharitonov and C.-S. Brès, "Isolator-free unidirectional thulium-doped fiber laser," Light: Science & Applications **4**, e340 (2015).
25. M. Chernysheva, C. Mou, R. Arif, M. AlAraimi, M. Rummeli, S. Turitsyn, and A. Rozhin, "High Power Q-Switched Thulium Doped Fibre Laser using Carbon Nanotube Polymer Composite Saturable Absorber," Scientific reports **6** (2016).
26. L. M. Zhao, D. Y. Tang, T. H. Cheng, and C. Lu, "Self-started unidirectional operation of a fibre ring soliton laser without an isolator," Journal of Optics A: Pure and Applied Optics **9**, 477–479 (2007).
27. D. Li, D. Shen, L. Li, H. Chen, D. Tang, and L. Zhao, "Unidirectional dissipative soliton operation in an all-normal-dispersion Yb-doped fiber laser without an isolator." Applied optics **54**, 7912–6 (2015).
28. K. Kieu and M. Mansuripur, "All-fiber bidirectional passively mode-locked ring laser," Opt. Lett. **33**, 64–66 (2008).
29. V. Mamidala, R. I. Woodward, Y. Yang, H. H. Liu, and K. K. Chow, "Graphene-based passively mode-locked bidirectional fiber ring laser," Opt. Express **22**, 4539–4546 (2014).
30. C. Zeng, X. Liu, and L. Yun, "Bidirectional fiber soliton laser mode-locked by single-wall carbon nanotubes," Opt. Express **21**, 18937–18942 (2013).
31. X. Yao, "Generation of bidirectional stretched pulses in a nanotube-mode-locked fiber laser." Applied optics **53**, 27–31 (2014).
32. V. Tsatourian, S. V. Sergeyev, C. Mou, A. Rozhin, V. Mikhailov, B. Rabin, P. S. Westbrook, and S. K. Turitsyn, "Polarisation dynamics of vector soliton molecules in mode locked fibre laser." Scientific reports **3**, 3154 (2013).
33. R. A. Sammut, "Range of monomode operation of W-fibres," Optical and Quantum Electronics **10**, 509–514 (1978).
34. S. Kawakami and S. Nishida, "Characteristics of a doubly clad optical fiber with a low-index inner cladding," IEEE Journal of Quantum Electronics **10**, 879–887 (1974).
35. M. Varnham, D. Payne, R. Birch, and E. Tarbox, "Single-polarisation operation of highly birefringent bow-tie optical fibres," Electronics Letters **19**, 246 (1983).
36. J. Simpson, R. Stolen, F. Sears, W. Pleibel, J. MacChesney, and R. Howard, "A single-polarization fiber," Journal of Lightwave Technology **1**, 370–374 (1983).
37. A. M. Kurbatov and R. A. Kurbatov, "Fiber polarizer based on W-lightguide Panda," Technical Physics Letters **37**, 626–629 (2011).
38. D. A. Nolan, G. E. Berkey, M.-J. Li, X. Chen, W. A. Wood, and L. A. Zenteno, "Single-polarization fiber with a high extinction ratio." Optics letters **29**, 1855–7 (2004).

39. L. Nelson, D. Jones, K. Tamura, H. Haus, and E. Ippen, "Ultrashort-pulse fiber ring lasers," Applied Physics B **65**, 277–294 (1997).
40. W. T. Silfvast, "Laser Fundamentals," (1997).

1. Introduction

Since their first demonstration, the ultrafast fibre lasers have been an object of continuous scientific and industrial research interest thanks to the highly integrated design and as a consequence compact size, lower cost, and excellent robustness against environmental exposure. All these practical advantages are highly desirable in the broad variety of the continuously developed application fields. Nowadays the range of ultrafast fibre lasers applications covers, but not limited to, micromachining, medical imaging, ophthalmology, location and precision metrology. In order to generate ultrashort pulses, most ultrafast fibre lasers utilise passive mode-locking technique, using saturable absorption phenomenon of optically induced transparency under intense laser light. Having picosecond or sub-picosecond absorption recovery time, saturable absorbers (SA) can modulate gain/losses in a laser cavity leading to the formation of sub-picosecond or femtosecond pulses. Commonly used SAs in fibre lasers are semiconductor saturable absorber mirrors (SESAM) [1], SWNTs [2, 3], graphene [4], transition-metal dichalcogenides (TMDs) [5]. The nonlinear optic Kerr-effect, i.e. the dependence of the refractive index on the intensity (peak power), has established another type of effective modulators with femtosecond time response. They are NPE [6], nonlinear optical and amplifying loop mirrors (NOLM and NALM) [7,8]. Besides, the benefits of the simultaneous use of two SAs with a different recovery time for the creation of hybrid mode-locking have been recently proved in several works [9–11], by demonstrating generation of ultrashort pulses with higher average power, temporal purity, and higher frequency stability.

The choice of SA determines the fibre laser configuration, such as ring, linear, figure-of-eight or others. However, the ring geometry is simple, does not require additional elements like mirrors in Fabri-Perot cavities and, therefore, can be easily assembled in all-fibre design. Moreover, the ring configuration presents the elegant solution to ensure bidirectional laser generation.

Bidirectional ultrafast lasers have gained substantial research and industrial interest for particular sensing applications, including precise rotation measurements in gyroscopy. The gyroscopic effect is explained using Sagnac theory, which assumes the different length of the optical pathways of counter-propagating pulses during the rotation [12]. Since the first demonstration, different works have demonstrated the gyroscopic effect in based on semiconductor diode [13], dye [12, 14], Nd:YVO_4 crystal [15], and fibre nonlinear loop reflector [16, 17]. However, only one work has been presented thus far on ultrafast bidirectional ring laser gyroscope [18], which demonstrate that there is room for future investigations to optimise the stability and enhance the sensitivity of rotation measurements, first of all by the improvement of the performance of isolator-free ring fibre laser configuration by itself.

An optical isolator is typically incorporated in the ring fibre laser with a principal function to suppress the uncontrolled cavity back-reflections, i.e. to ensure unidirectional operation, and to enhance the mode-locking regime by decreasing the self-starting threshold [19]. The operation principle of the optical isolator is based on Faraday effect. The orthogonally polarised components of an input beam are separated in the first polariser; a Faraday rotator ensures a particular, usually 45, rotation angle of polarisation direction for both components; whereas the second polariser combines two elements together. In the case of the backward-propagating beam, the second polariser would not combine polarisation components, but will cause an offset beam position, launching the beam into an internal absorber [20, 21].The optical isolators have a complicated configuration with free-space optics and possess limited bandwidth of tens nanometres, obstructing the tuneability of laser systems. Development of mode-locked fibre

lasers without optical isolators opens avenues for highly tuneable, cost-effective and veritably fibre integrated solutions. In [22–24] lasers were built in modified ring fibre laser cavities so-called theta or Yin-Yang cavity, which features S-shaped feedback. The feedback determines non-reciprocal losses in the cavity, and, therefore, favoured and suppressed directions of laser generation. The same setup was also studied in pulse regime operation [23, 25]. In the case of isolator-free ultrafast fibre lasers, both quasi-unidirectional and bidirectional generation have been experimentally demonstrated. For instance, in the lasers mode-locked by NPE the bidirectional generation could be achieved only bellow the mode-locking threshold, during continuous wave operation. As soon as the mode-locking was initiated, one of the directions dominates over another, giving, therefore, an isolator-free quasi-unidirectional generation with net extinction ratio around 10 dB [26, 27]. Such behaviour refers to NPE mode-locking when the role of the nonlinearity-induced directional symmetry breaking is high. The stable bidirectional operation has been demonstrated in fibre lasers mode-locked by SWNT-based or graphene SA [28–31].

In this paper, we propose isolator-free ultrafast erbium-doped fibre laser, operating in both CW and CCW unidirectional and bidirectional regimes. The laser is hybrid mode-locked using SWNT-PVA SA and NPE. The SWNT-PVA, refereed in this case as to comparatively slow saturable absorber (relaxation time is 300-700 fs), is used for mode-locking initiation. The NPE features relaxation time in order of 10 fs and therefore, ensures efficient pulse narrowing and overall stabilisation of generation. Moreover, as shown in previously published works, acting separately the SWNT saturable absorber enables stable bidirectional generation, whereas the NPE guarantees unidirectional operation. Simultaneous application of these two saturable absorbers allows to achieving easy switching between generation directions. The switching between regimes with different generation directions can be achieved by adjusting the intracavity birefringence, controlling the SOP. Our result will stimulate the development of switchable fibre laser devices for the rotation sensitive applications, sensing and imaging enabling simultaneous two different types of measurement, such as confocal imaging, pump-probe and total internal reflection fluorescence microscopy.

2. Experimental setup

We used commercially available purified SWNTs purchased from Unidym (Lot P0261) as initial material to fabricate the SWNT- Polyvinyl Alcohol (PVA) composite[34]. Two mg of SWNT powder was dispersed in 10 ml of deionized (DI) water in the presence of 10 mg of Sodium dodecylbenzene sulfonate surfactant (SDBS). The dispersion was then ultrasonicated for 1 hour at 20 kHz and 200 W using a NanoRuptor (Diagenode) processor. The dispersion was placed into MLS 50 rotor and centrifuged at 25K RPM during one hour with Beckman

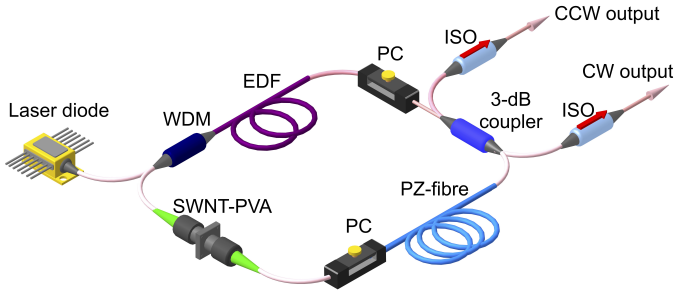

Fig. 1: Schematic setup of the isolator-free ring Erbium-doped hybrid mode-locked fibre laser

Optima Max-XP ultracentrifuge in order to remove impurities and residual bundles. After centrifugation process, the resultant solution was mixed with PVA and poured in the Petri dish. The SWNT-PVA standing film was then obtained after drying the sample in the desiccator. The film has a homogeneous distribution of SWNTs on a submicron scale, as confirmed by optical microscopy. The sample possesses high optical absorption density about 0.85 at the erbium-doped operation wavelength band around 1550 nm due to the presence of tubes with diameters of 1.2 nm [32]. The sample features high modulation depth around 54%. Hence, the non-saturable losses are also high - 46%. The saturation intensity of the SWNT-PVA film is 58.8 MW/cm^2.

The laser setup is presented in Fig. 1. The 2-m erbium-doped fibre (Liekki Er30-4/125) is pumped via FBG stabilised laser diode at 980 nm trough 980/1550 wavelength division multiplexor (WDM). The erbium-doped fibre has a nominal group velocity dispersion (GVD) of β_2 = 12.5 ps^2/km at 1.44 μm. The active fibre features a 6.5 μm mode field diameter with λ_c = 890 nm cut-off wavelength. The non-saturated absorption at 980 nm pumping wavelength is 6.5 dB/m. The laser is operating in the hybrid mode-locking regime with NPE and the SWNT-PVA film. The SWNT-PVA sample is sandwiched between optical fibre ferules. The NPE is realised by polarising optical fibre (HB1550Z from Thorlabs) and a pair of polarisation controllers [11]. The polarising fibre is made in the so-called bow-tie geometry. Such a configuration enables modification of the optical fibre refractive index due to the stress-induced birefringence and, therefore, leads to the shifting the cut-off wavelength for the orthogonally polarised fibre modes. As a result, orthogonally polarised (slow and fast) HE_{11} modes have significantly separated cut-off wavelengths and undergo considerably different attenuations [33, 34], and the polarising fibre supports single-polarization light propagation. Apart from the bow-tie geometry, first introduced in [35], the polarising effect can be realised by the W-type refractive index optical fibres [33, 34], optical fibres with elliptical depressed inner cladding [36], so-called PANDA technology (with boron-silicate stress-inducing rods) [37], and by a dual-hole fibre configuration [38]. The fibre used in our experiment, having the length of 6 m and being coiled in 9 cm diameter, provides the extinction ratio of 30dB within the bandwidth of $\sim$130 nm.

The laser pump power threshold is 35 mW when the laser operates in continuous wave regime. With the pump power increase to 60 mW, the laser starts to operate in a Q-switched regime with mode-locked modulations in both directions. Though by adjusting the polarisation controller, the mode-locked generation can be achieved. The pulse repetition rate is $\sim$10.99 MHz, which is in good agreement with the fundamental frequency of the cavity with the length of 18 m. Corresponding pulse repetition period is 91 ns. We used EXFO Power Meter PM-1100 for output power measurements, optical spectrum analyser ANDO AQ6317b with the measurement range of 600-1750 nm and a resolution of 0.05 nm, RF spectrum analyser Agilent 8562A with 100 Hz resolution bandwidth, the autocorrelator from Avesta (AA-20DDR), and oscilloscope Le Croy (WJ352A) with the sample rate up to 2 GS/s. We have also used in-line polarimeter (Thorlabs IPM5300, 1 μs resolution, 1024 samples) to analyse SOP evolution for different regimes.

3. Experimental results

3.1. Unidirectional operation

At first, laser tends to operate in a counter-clockwise (CCW) direction. At the pump power of 75 mW, the output power of the CCW direction is 1.1 mW, whereas the output power of the CW direction is only 20 μW. Therefore, we can conclude that the laser operates in a quasi-unidirectional generation with the net extinction ratio of 17.4 dB. Fig. 2 presents the output parameters in the case of dominating CCW direction. The spectra of both CW and CCW directions, centred at 1558 nm, feature the similar shape with the bandwidth at the 3-dB level of 6.6 and 4.6 nm, correspondingly, and identical position of Kelly side-bands, proving soliton

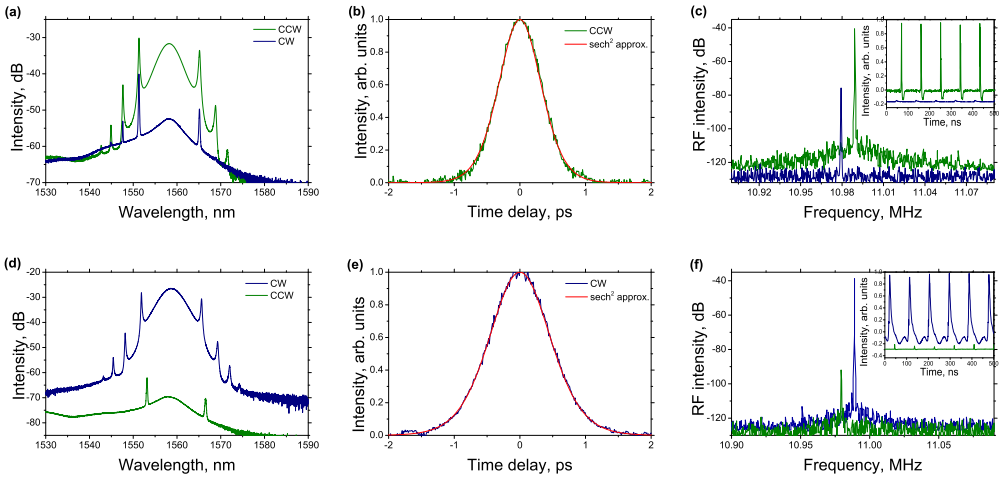

Fig. 2: Mode-locked laser output parameters at dominating CCW (a-c) and CW (d-f) directions: a,d) Output spectra for CW and CCW; b,e) Autocorrelation traces of dominating direction; c,f) RF spectra of dominating direction. Insets: CW and CCW pulse trains

generation in both directions (Fig. 2a). According to the phase-matching condition, sidebands of the soliton occur at the frequency offset $\Delta\omega$ [39]:

$$\Delta\omega = \pm\frac{1}{\tau}\sqrt{m\frac{8Z_0}{Z_p} - 1} \tag{1}$$

here, m - is an integer order of sidebands, Z_p - is the perturbation length (length of the laser), Z_0 - is the soliton period. Due to the low output power of CW direction, the autocorrelation trace was measured only in CCW and presented in Fig. 2b. The pulse duration τ, in this case, is about 500 fs. However, taking into account Eq. 1 we can assume that the counter-propagating pulses feature similar duration.

The time-bandwidth product of the generated pulse $\Delta\nu\cdot\Delta\tau$ = 0.315. This value is typical for transform-limited soliton pulses. The green plot in Fig. 2c demonstrates the 65 dB signal-to-noise ratio of the fundamental frequency of the RF spectrum of the CCW direction. The suppressed CW direction has a smaller signal-to-noise ratio of only 40 dB, whereas at longer scale generation on sub-frequencies was also observed. Due to high power difference between the CW and CCW directions, the nonlinear refractive index for the counter-propagating pulses is not the same. Generally, the repetition rate of regularly spaced train of pulses in ring mode-locked laser output can be found as: $f_{rep} = c/(L\cdot n)$, where L - is the cavity length, c is the speed of light in the vacuum and n is the refractive index of the medium where light propagates [40]. According to the nonlinear optical Kerr-effect the refractive index n consists of linear n_0 and second-order nonlinear refractive index n_2: $n = n_0 + n_2 \cdot I$ [40], where n_2 = $2.87\cdot10^{-16}$ cm^2/W for silica fibres at $\sim$1560 nm wavelength range. Therefore, having different intensities the CCW and CW directions generate with different fundamental frequencies: 10.989 and 10.979 MHz, correspondingly. The inset in Fig. 2c shows pulse trains of CW and CCW directions. The laser pulse trains in CW and CCW directions were detected simultaneously using correspondingly EOT (ET-5000F) and New Focus photodetectors with the bandwidths of 12.5 and 1 GHz. As it seen in the inset, the CW pulse train is shifted over the CCW one.

With the precise adjusting of the PCs in the laser cavity, the generation direction can be

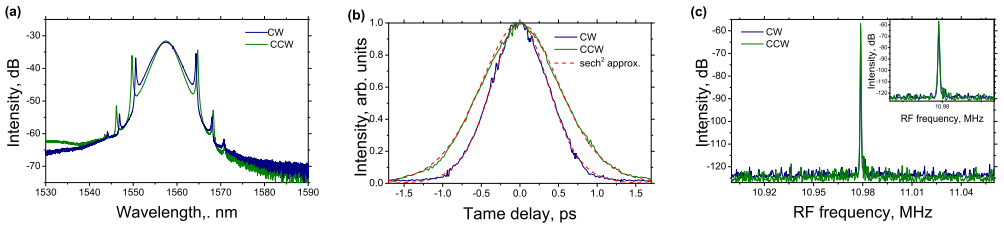

Fig. 3: Bidirectional mode-locked laser output parameters for CW and CCW directions: a) Output spectra; b) Autocorrelation traces of dominating direction; c) RF spectra of dominating direction. Inset: CW and CCW pulse trains

altered at the same level of the pump power. With the CW direction domination, the power of CW output reaches 2.68 mW, whereas the CCW output power decreases to 16 μW, giving the unidirectional isolation of at least 22 dB. The laser output parameters are presented in Fig. 2. The spectra are centred at 1559 nm and feature the bandwidth of 4.16 and 4.55 nm for CW and CCW pulses, correspondingly. The pulse duration in CW direction is 680 fs. This allows estimation of the time-bandwidth product of CW pulses as 0.35, which is negligibly larger than the well-known value of transform-limited soliton. The signal-to-noise ratio of the RF spectrum of favoured CW channel is 74 dB, whereas the suppressed CCW direction features only 20 dB (Fig. 2f). Analogous to the previous case the CW and CCW fundamental frequencies have the difference of about 10 kHz. The inset in Fig. 2f presents the pulse trains of both generation directions.

3.2. Bidirectional operation

Further adjustment of the polarisation controllers enables bidirectional mode locking. In this case, when the SOP was fixed, the bidirectional generation was self-starting and demonstrated excellent stability in laboratory conditions. The average optical powers are 1.17 and 1.11 mW, respectively for the CW and CCW trains. The CW and CCW directions feature different output power due to the asymmetrical position of the active fibre, SA and output coupler as well as unidirectional pumping configuration. This creates unevenly distributed losses and gain in the cavity. CW pulse is coupled output directly after amplification, whereas the CCW pulse propagates through the SA before it is gated out. Figure 3a demonstrates spectra of the counter-propagating pulses with the bandwidth at the –3dB level of 3.76 and 4.71 nm for CW and CCW directions, respectively. Autocorrelation traces confirm the single-pulse generation of the bidirectional operation. The autocorrelation traces in Fig. 3b show pulse durations of CW and CCW pulses of 790 and 570 fs, correspondingly. Such durations assume that both pulses are slightly chirped (time-bandwidth products: 0.37 for CW, 0.335 for CCW). The RF spectra show more than 65 dB signal-to-noise ratio for both generation directions. The difference in the parameters of counter propagating pulses can be explained with the strictly different evolution of beams transmitted inside the fibre ring. The normal dispersion erbium-doped gain fibre is placed asymmetrically in respect to output coupler, creating dispersion and nonlinearity-imbalanced cavity. Therefore, the counter-propagating beam acquire different intensity-dependent phase shift and frequency chirp.

3.3. Polarisation measurements

A polarimeter IPM5300 (Thorlabs) with 1 μs resolution and the range of 1 ms (99–99000 round trips) has been used to measure the normalized Stokes parameters s_1, s_2, s_3 and the degree of

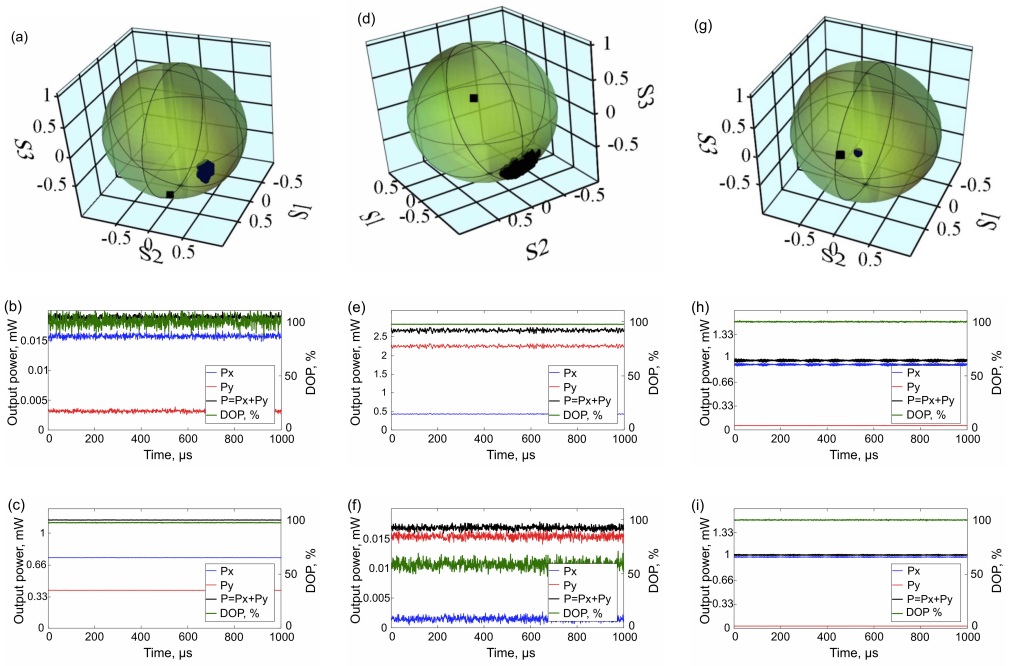

Fig. 4: Polarization dynamics in terms of the normalized Stokes parameters (a, d, g), DOP and output powers for the orthogonally polarized modes (b,c, e,f, h,i) for the unidirectional (a-f) and bidirectional (g-i) operations. Notations: a) CCW dominating channel (squares); CW suppressed channel (dots); b) DOP and output powers for suppressed CW channel; c) DOP and output powers for favoured CCW channel; d) CW dominating channel (squares), CCW - suppressed channel (dots); e) DOP and output powers for favoured CW channel; f) DOP and output powers for suppressed CCW channel; g) CCW channel (squares), CW Channel (dots); h) DOP and output powers for CW channel; i) DOP and output powers for CCW channel.

polarization (DOP) which depends on the output power of a two linearly cross-polarized SOPs P_x, P_y and the phase difference between them $\Delta\phi$ as follows:

$$S_0 = P_x + P_y, S_1 = P_x - P, S_2 = 2\sqrt{P_x P_y} cos\Delta\phi, S_3 = 2\sqrt{P_x P_y} sin\Delta\phi$$
$$s_i = \frac{S_i}{\sqrt{S_1^2 + S_2^2 + S_3^2}}, DOP = \frac{\sqrt{S_1^2 + S_2^2 + S_3^2}}{S_0}, (i = 1,2,3) \quad (2)$$

Application of in-line polarization controllers along with polarimeter helped to adjust the output SOPs for bidirectional and unidirectional operations and to lock it at elliptical one as shown in Fig. 4. The bidirectional regime provides almost coinciding SOPs and output powers whereas unidirectional regimes have asymmetrical properties for leading CW and CCW channels. Resulting stable degree of polarization (DOP) of 100% justifies high stability of SOPs for bidirectional (Fig. 4h,i) and unidirectional regime with leading CCW channel (Fig.4c). Unlike this, DOP of 60% for suppressed CCW channel (Fig. 4f) is the evidence of the fast evolution of SOP leading to a small perturbation of the leading CW channel (Fig. 4e) in the context of output power. As follows from the Fig. 4 and previous discussion, mapping the different regimes in the context of the SOP stability and high DOP can be used for optimal adjustment of the laser

to get the stable operation in the context of signal-to-noise ratio, output power and femtosecond pulse width.

4. Conclusion

In summary, we have experimentally demonstrated isolator-free erbium-doped ring fibre laser hybrid mode-locked by SWNT saturable absorber and NPE, which strongly impact on a switching of the lasing direction in the laser. The NPE introduces polarisation sensitivity of the cavity and, hence, allows efficient tuning of the non-reciprocal losses for counter-propagating pulses and suppresses their interaction. The SWNT-PVA SA, in its turn, maintains bidirectional generation.

Depending on the net birefringence of the cavity, we achieved extinction ratio up to 22 dB between the favoured CW and suppressed CCW generation directions and 13 dB vice versa. The output parameters of both regimes of unidirectional generation are competitive with those of ring cavities with isolator. In both cases, the laser generates near transform-limited soliton pulses with the duration of 680 and 500 fs and output power 2.68 and 1.1 mW at pump power level of 75 mW, respectively in CW and CCW dominating direction.

We, therefore, anticipate that the demonstrated fibre laser system will become a basis for the development of a stable and cross-functional ultrafast laser source with advanced capability. The switching mechanism between generation directions allows a single laser to operate as two separate femtosecond lasers simultaneously. Such ability can find application in imaging techniques and sensing, dramatically reducing the price of the final measurement system. In the meantime, the demonstration of the same laser setup operating in bidirectional regime will open ground for ultrafast fibre laser applications in rotation sensing technologies.

Acknowledgments

The support by the Marie-Curie Inter-national Research Staff Exchange Scheme "TelaSens" project, Research Executive Agency Grant No 269271, Programme: FP7-PEOPLE-2010-IRSES and the European Research Council through the FP7-IDEAS-ERC grant ULTRALASER is gratefully acknowledged. M. C. acknowledges the support of EU Horizon2020 Marie S.-Curie IF MINDFLY project. The authors thank Dr A. Krylov from the FORC RAS for fruitful discussion.